World Journal of Agricultural Research, 2018, Vol. 6, No. 4, 153-166
Available online at http://pubs.sciepub.com/wjar/6/4/6

DOI:10.12691/wjar-6-4-6

Evaluating the Association between Climate Variability and Vegetation Dynamics by Using Remote Sensing Techniques: The Case of Upper Awash Basin, Ethiopia

Getachew Bayable Tiruneh[1,*], Berhan Gessesse[2], Tulu Besha[3], Getachew Workineh[4]

[1]Department of Land Administration and Surveying, Oda Bultum University, Chiro, Ethiopia
[2]Remote Sensing Research Division, Entoto Observatory and Research Centre, Addis Ababa, Ethiopia
[3]Geodesy Research Division, Entoto Observatory and Research Centre, Addis Ababa, Ethiopia
[4]Department of Geography and Environmental Science, Debre Tabor University, Debre Tabor, Ethiopia
*Corresponding author: bayable.geta@gmail.com

Received November 17, 2018; Revised December 18, 2018; Accepted December 28, 2018

Abstract Examining the impact of climate variability on vegetation dynamics is the missing research element in Upper Awash Basin. Hence, the aim of this study was investigating climate variability and their impacts on vegetation dynamics. Monthly 250 meter resolution Moderate Imaging Spectro-radiometer (MODIS) Normalized difference vegetation Index (NDVI), 1kilometer resolution MODIS Land Surface Temperature (LST), rainfall data from 19 meteorological stations, and NINO3.4 (SSTA) were used for this study. A Mann Kendall (MK) trend test was used to determine the trend of each dataset using seasonal and annual time-series. Pearson correlation coefficient was also used to estimate the association between NDVI and climatic elements. Results of this study revealed that there was no significant change in the annual and seasonal NDVI, LST, Sea surface Temperature Anomaly (SSTA) and rainfall during the period 2001 to 2016, except NDVI in belg season. The correlation between NDVI and rainfall was positive (r = 0.51), strong positive (r= 0.62), low positive (r = 0.45) and low negative (r = -0.33) for annual, belg, bega and kiremit seasons, respectively. Similarly, the correlation between NDVI and LST was negative (r = - 0.58), strong negative (r= -0.67), negative (r = -0.5) and low positive (r = 0.41) for annual, belg, bega and kiremit seasons, respectively. On the other hand, the correlation between NDVI and SSTA was low negative (r = - 0.41), weak negative (r= -0.29), weak positive (r = 0.22) and low positive (r = 0.42) for annual, bega, belg as well as kiremit seasons, respectively.

Keywords: *climate variability, LST, NDVI, RF, SSTA, upper awash basin*

Cite This Article: Getachew Bayable Tiruneh, Berhan Gessesse, Tulu Besha, and Getachew Workineh, "Evaluating the Association between Climate Variability and Vegetation Dynamics by Using Remote Sensing Techniques: The Case of Upper Awash Basin, Ethiopia." *World Journal of Agricultural Research*, vol. 6, no. 4 (2018): 153-166. doi: 10.12691/wjar-6-4-6.

1. Introduction

Climate variability is one of the most determinant factors affecting vegetation condition. There is a strong association between climate and vegetation dynamics [1]. The variability in climate directly causes change in the ecosystem [2,3]. Other studies also revealed the significant effect of climate variability on the natural environment [4,5]. Vegetation coverage has exhibited the most sensitive response to climate variability [6]. This is due to the fact that vegetation in terrestrial ecosystems is considered as an intermediate link among the biosphere and atmosphere of the earth system. Vegetation dynamics and their relationship with climate variability have become a hot issue at global level [7]. Climate plays a major role in vegetation phonological cycles. Vegetation growth is functionally dependent on climate. Consequently, a change in biophysical parameter of vegetation canopy implies a change in climate; accordingly vegetation is used as key inputs into many climate change models [8].

Remote sensing plays an important role in providing an effective tool for monitoring different parameters of complex ecosystems [9] in many countries like Ethiopia. Satellite based vegetation index derivation is one of the research approaches to assess climate variability and vegetation dynamics of the earth's surface [10,11]. Satellite data are increasingly used to investigate the association between vegetation indices and climatic parameters [12]. Normalized Difference Vegetation Index (NDVI) derived from Coarse to moderate-scale satellite image products is considered as reliable indicators of vegetation conditions and a proxy of biomass production at regional scale [13].

Climate variability is the most important cause of food insecurity in many part of the world [14]. Hence, it has recently become a pressing issue in various development,

environment, and political forums at national, regional and international levels [15]. In Ethiopia, El Niño has been the cause of crop failure, livestock death and food insecurity for many years. Since, the rainy season in Upper Awash Basin, mostly dependent on El Niño and La Niña events occurring in the Tropical Pacific Ocean [16]. Analyzing El Niño/La Niña Southern Oscillation episodes together with other climatic parameters would be helpful for many sectors. However, very limited studies have been conducted to assess the impact of El Niño/La Niña Southern Oscillation episodes with other climatic parameters on vegetation spatio-temporal dynamics in Ethiopia in general and in the Upper Awash Basin in particular. A recent study conducted by [17] which focus on spatio-temporal variability of vegetation cover and main climatic elements with El Niño Southern Oscillation (ENSO) in north western Ethiopia using geoinformation techniques revealed an increase in kiremit and belg seasonal vegetation coverage during El Niño episodes contrasted to La Niña episodes. However, there has been a rainfall delay during El Niño episodes in the first one or two months of kiremit season. The association between main climatic elements (rainfall and temperature) and vegetation dynamics associated with ENSO has not been investigated in the study area. Therefore, this study was aimed at investigating the association between climate variability and vegetation dynamics using remotely sensed vegetation products/indices and in-situ meteorological observations in the Upper Awash Basin, Ethiopia.

2. Materials and Methods

2.1. Study Area

This study was conducted in the Upper Awash Basin, Ethiopia. It is located between 8°16'N - 9° 18' N and 37° 57'E - 39°17'E. It covers a total area of 10,640.1 km^2.

2.2. Data Types and Sources

This study used in-situ meteorological data obtained from the Ethiopian National Meteorological Agency (NMSA) and satellite data acquired from the United States Geological Survey (USGS). Weather stations were chosen based on data availability and their spatial distribution within the study area. However, spatial location of stations that records temperature data was distributed unevenly in the study area and most stations recorded only rainfall data. Due to this, the study used MODIS Land Surface Temperature (LST) data instead of using in-situ temperature data from National Metrological Agency (NMA).

2.2.1. Meteorological Dataset Preparation

The meteorological dataset was checked for its spatial and temporal completeness prior to subsequent analysis. On top of this, the quality of these data was assessed and missing values were replaced by the long-term mean for the missing month [18].

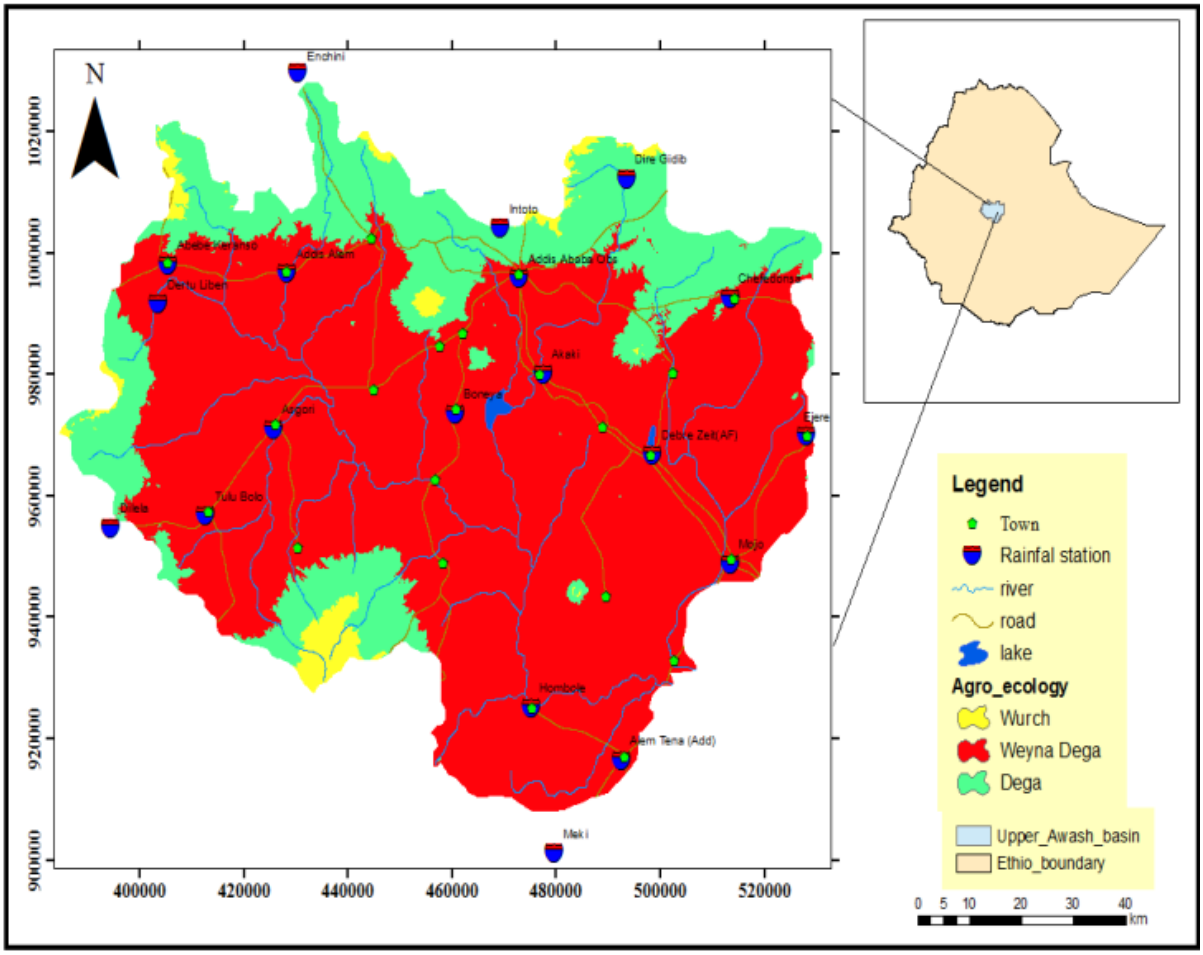

Figure 1. Location map of the Upper Awash Basin

In this study, surface map in the form of grid map of precipitation for the study area was constructed using the geostatistical interpolation method known as ordinary kriging [17]. Ordinary kriging relies on spatial correlation structure of the data to determine the weighting values instead of weighting nearby data points by some power of their inverted distance and it is an effective spatial interpolation and mapping tool. Because it honors data locations provides unbiased estimates at unsampled locations and provides for minimum estimation variance. It is best linear unbiased estimator [19,20,21]. Ordinary kriging is found to be the best method as it produces little root mean square error [21,22]. More importantly, ordinary krigging technique enables to see the semivariogram plots and probability maps to ascertain the model fit of prediction function [19] and to have a clue on the interpolation error [23].

$$\acute{Z}(S_o) = \sum_{i=1}^{N} (\lambda_i Z(S_i)) \quad (1)$$

where Z(Si) is the measured or computed value (for the purpose of this study, rainfall) at i^{th} location λi is an unknown weight for the measured value at the i^{th} location, is the prediction location while N is the number of locations where rainfall is measured.

In addition to this, mean sea surface temperature (SST) anomalies of NINO3.4, NINO3 and NINO4 region from National Oceanic and Atmospheric Administration (NOAA) satellite mission was used for the analysis to understand the association between SST anomalies and NDVI, and between SST anomalies and rainfall in the Upper Awash Basin. Since NINO 3.4 has characteristics of both NINO3 and NINO4, researchers such as [24] and [25] recommended to use NINO3.4 SST anomalies. Hence, the study has used SST anomalies of NINO3.4 region. To be classified as a full-fledged El Niño and La Niña episode the NINO3.4 SST anomalies must exceed +0.5 for El Niño and less than - 0.5 for La Niña.

2.2.2. Remote Sensing Data

This study used sixteen days MODIS composites (MOD13Q1) MODIS NDVI (250 m) and 8 days composites (MOD11A2 LST (1 km)) time series for time scale from 2001 to 2016. The MODIS 250 m NDVI product (MOD13Q1) of 16-day composites provided vegetation phenology data. MODIS which was launched on NASA's earth observing system (EOS) is the most important sensor for monitoring the terrestrial ecosystem [26]. It is more sensitive to changes in vegetation dynamics and was found to be a more accurate and versatile instrument to monitor the global vegetation conditions than the AVHRR [26,27]. This study has primarily used MODIS NDVI data as an indicator for providing vegetation properties and associated changes for large spatial scale [17,28]. NDVI is derived from MODIS bands 1 and 2 as shown below:

$$NDVI = \frac{B2 - B1}{B2 + B1} \quad (2)$$

Where B1 and B2 are the reflectance values yielded by the MODIS band1 (red) and band 2 (near infrared), respectively.

2.2.3. Re-projection, Format Conversion and Preprocessing of MODIS Datasets

MODIS products are provided with hierarchical data format (HDF), which is not as such compatible to easily read and undertake analysis of the vegetation phenology and LST data using remote sensing related software packages In addition to this, the data is archived with global sinusoidal projection system which requires appropriate coordinate transformation and projection to use the data for regional and local applications with other spatial datasets. Therefore, coordinate transformation and format conversion is undertaken by using MODIS Reprojection Tool (MRT), which is open source geospatial software product.

MODIS NDVI and LST datasets are composite products produced by maximum value compositing (MVC). As a result datasets inevitably contain disturbances caused by some errors such as atmospheric variability [29], aerosol scattering [30] and some residual errors [31]. These disturbances degrade the data quality and add considerable uncertainty to temporal sequences, confusing the analysis of temporal image sequences by introducing significant variations on the NDVI and LST time series data. Noise reduction or fitting a model to observation data is required before temporal analysis. Though, there are many types of smoothing algorithms [32-38], for this study, Fast Fourier Transform (FFT) algorithm [36,38] was adopted. FFT is considered as a powerful tool to reproduce NDVI and LST time series [36,38] and computes Discrete Fourier Transform (DFT) in a very quick way. Fast Fourier Transform algorithm was used for the purpose of screening and removal of cloud contaminated observations and temporal interpolation of the remaining observations to reconstruct gapless images at a prescribed temporal scale [36,38].

2.2.4. Trend Analysis

Long term NDVI and climatic element trends are good indicator to assess the existence of any associated changes in vegetation productivity and climatic element variability [39]. This study used non-parametric statistical tests, the Mann-Kendall trend test to evaluate the statistical significance of trends [40,41,42,43] using XLSTAT 2017. Unlike ordinary least squares regression, the Mann-Kendall trend test is less affected by missing values and uneven data distribution, and are robust towards extreme values and serial dependence [44]. To identify the magnitude of trend, Sen's slope has been calculated [43,45,46] which is a form of robust linear regression and less affected by gross data errors or outliers compared to linear regression analysis [47].

The Mann-Kendall test analyzes the sign of the difference between later measured data and earlier measured data. Each later measured value is compared to all values measured earlier; resulting in a total of n (n-1)/2 possible pairs of data, where n is the total number of observations. To perform a Mann-Kendall test, compute the difference between the later-measured value and all earlier-measured values, (yj-yi), where j>i, and assign the integer value of 1, 0, or −1 to positive differences, no differences, and negative differences, respectively. The test statistic, S, is then computed as the sum of the integers:

$$S = \sum_{i=1}^{n-1} \sum_{j=i+1}^{n} sign(yj - yi) \quad (3)$$

where sign (yj-yi), is equal to +1, 0, or -1 as indicated above [47]. When *S* is a large positive number, later-measured values tend to be larger than earlier values and an increasing/positive trend is indicated. When S is a large negative number, later values tend to be smaller than earlier values and a downward trend is indicated. When the absolute value of S is small, no trend is indicated. The rate of change can be calculated using the Sen Slope estimator [48]

$$\beta 1 = median\left(\frac{yj - yi}{xj - xi}\right). \quad (4)$$

For all i < j and i = 1, 2, …, n-1 and j = 2, 3,…, n; in other words, computing the slope for all pairs of data that were used to compute S. The median of those slopes is the Sen slope estimator.

2.2.5. Correlation Analysis

This study used Pearson Correlation Coefficient to test for a linear relationship between NDVI and climatic elements (temperature, precipitation or SST anomalies), and also between SST anomalies and Rainfall. The Pearson correlation coefficient is a measure of the linear relationship between two variables X and Y, giving a value between +1 and -1 inclusive, where 1 is total positive correlation, 0 is no correlation, and -1 is negative correlation. It is widely used in the science field as a measure of the degree of linear association between two variables [49]. Methematically, it can be presented as follows;

$$r_{xy} = \frac{\sum_{i=1}^{n}(Xi - Xm)(Yi - Ym)}{\sqrt{\sum_{i=1}^{n}(Xi - Xm)^2 \sum_{i=1}^{n}(Yi - Ym)^2}} \quad (5)$$

where r_{xy} is the simple correlation coefficient of variables X and Y, Xi is NDVI or SST anomalies of the i^{th} year/month, Yi is climatic elements (temperature, precipitation or SST anomalies) of the i^{th} year/month; Xm is the average NDVI or SST anomalies for all years/month, Ym is the average temperature, precipitation or SST anomalies for all years/month [50,51].

3. Results and Discussion

3.1. Temporal Changes of Mean Annual (NDVI), (LST), (SSTA) and Rainfall (RF) Value for Upper Awash Basin

The mean annual estimates of NDVI, LST, SSTA and RF have exhibited temporal variability over the study period (2001-2016). For instance, LST has a gradient of 2.77°C; the lowest LST is 28.96°C in 2010 and the highest LST is 31.73°C in 2015. From the perspective of vegetation dynamics, the NDVI has the lowest mean annual value of 0.39 in 2012 and 2015, and highest value of 0.43 in 2001 (Figure 2a). In Upper Awash Basin, the mean annual estimates of NDVI and LST computed over a period of 16 years correspond to 0.41 and 30.16°C, respectively. Change curves of annual mean NDVI and annual mean LST has been fluctuated in opposite direction i.e as the value of LST increases, NDVI value decreases and vice versa during the study period. Besides, the change curves of annual mean NDVI and annual mean RF were fluctuating almost in the same direction i.e as the change curve of RF increases, NDVI curve also increases (Figure 2b). As described by [52] the NDVI value was highly dependent on the seasonal rainfall and low NDVI value was indicator of drought in the northwestern Ethiopia. As indicated in Figure 2c, the two variables, SSTA and RF, are observed to exhibit out-of-phase inter-annual oscillation patterns on time scale. SSTA has the highest and lowest annual mean values of 1.58 (in 2015) and -0.83 (in 2010), respectively. Although, RF has the highest and lowest mean annual estimates of 96.19 mm (in 2010) and 66.24 mm (in 2002), respectively. Change curves of annual mean RF and annual mean SST Anomalies were fluctuating in opposite direction i.e as the change curve of SST Anomalies increases, RF curve decreases and vice versa. According to [53], the main reason for inter annual variations of rainfall and the NDVI series is the Pacific El Niño/Southern Oscillation event, which reaches Ethiopia with a time lag of a few months. Similarly, change curves of annual mean NDVI and annual mean SST Anomalies were fluctuating almost in opposite direction i.e as the change curve of SSTA increases, NDVI curve decreases and vice versa (Figure 2d).

Undertaken Mann Kendall trend test indicates that overall mean annual values of NDVI and SST Anomalies have declined by 0.001 and 0.001°C per year, respectively (Table 1). The ρ-value of the mean annual NDVI and SSTA is 0.228 and 0.965, respectively. This indicates that the ρ-values are greater than the significance level α (0.05), suggesting that no significant decrement is observed in the mean annual estimates of NDVI and SST Anomalies at statistical confidence level of 95 %. On the contrary, the LST and RF have showed an increment in their mean annual estimates by 0.006°C and 0.064 mm per annum, respectively. The mean annual values of LST and RF have a ρ-value of 0.825 and 1.0, respectively. These ρ-values are greater than the significance level α (0.05) and this suggests that the increment in the mean annual values of LST and RF is not significant with the confidence level of 95 % over the study period. This indicates that, Upper Awash Basin is experiencing highly fluctuating climatic variables pattern than its change dimension [54]. This result is supported by findings reported by [55] and he has confirmed the absence of statistically significant trend for NDVI and rainfall in Addis Ababa and Debre Zeit (which are parts of our study area) from 1982 to 2006. Other studies also support the results of our study. For instance, [56] indicated that annual rainfall variability over northwestern Ethiopia has no trend he used rain gauge data to justify this. Besides, [57] showed that there was no trend in annual rainfall in north western dryland of Ethiopia (particularly Kaftahumera) over a period of 1983 to 2014, except the existence of trend in the seasonal variability of rainfall.

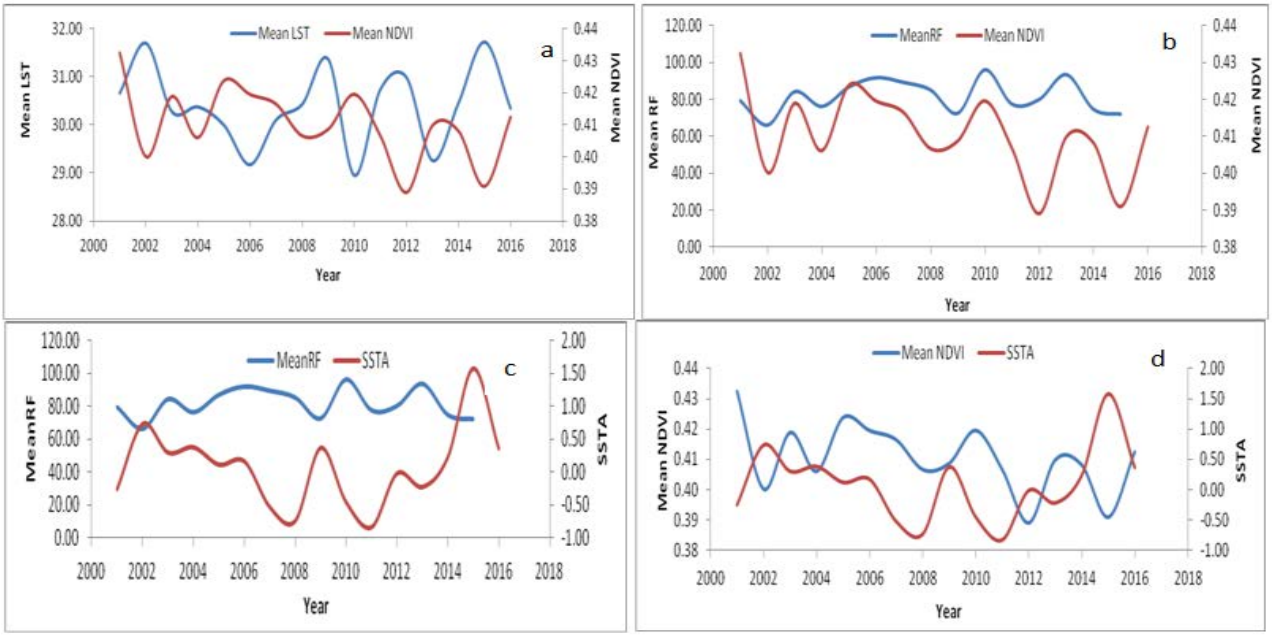

Figure 2. Variation of annual mean LST, NDVI, RF and SSTA of the Upper Awash Basin from 2001 to 2016

Table 1. Results of the Mann-Kendall trend test for annual mean NDVI, LST, SSTA and RF value for Upper Awash Basin.

	Kendall's *tau*	S	*ρ*-value (Two-tailed)	Alpha	Sen's Slope
Mean NDVI	-0.233	-28.000	0.228	0.05	-0.001
Mean LST	0.050	6.000	0.825	0.05	0.006
Mean RF	0.010	1.000	1.000	0.05	0.064
Mean SSTA	-0.017	-2.000	0.965	0.05	-0.001

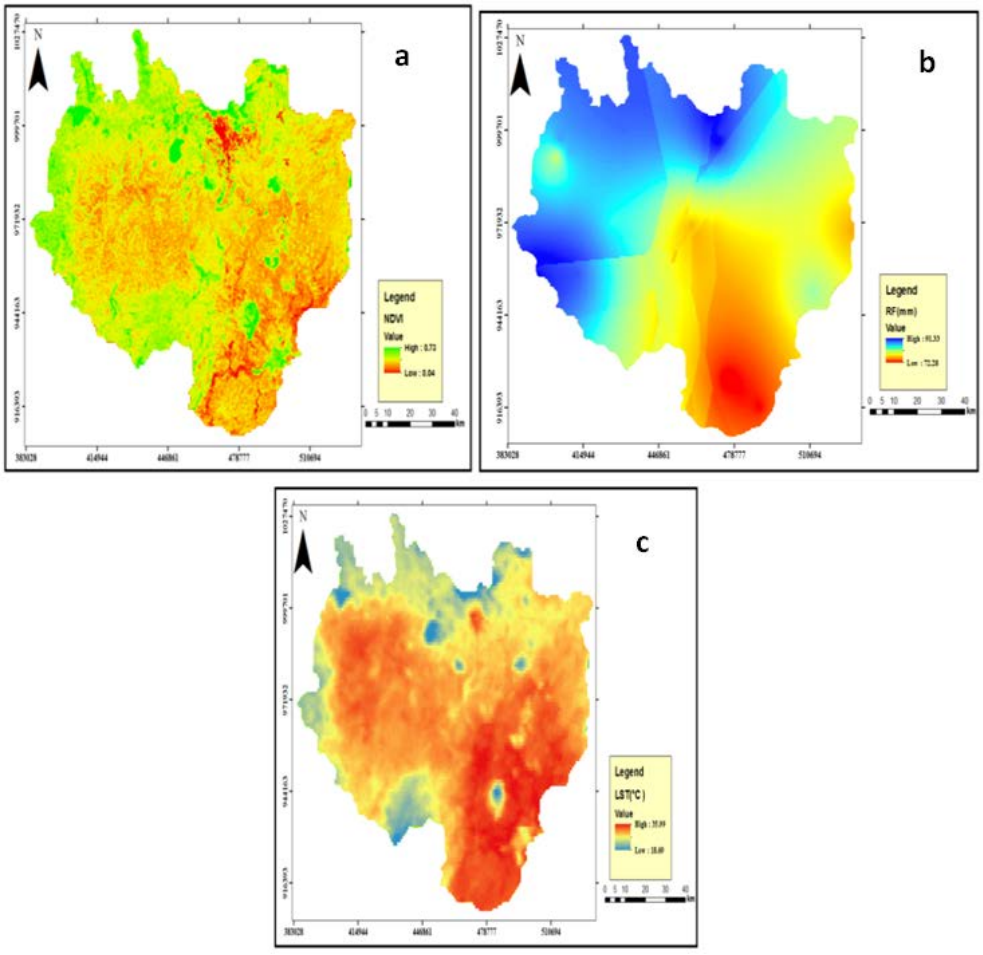

Figure 3. Spatial distribution of the Annual Average NDVI (2001-2016) (a), Annual Average RF (2001-2015) in mm (b) and Annual Average LST (2001-2016) in °C (c)

3.2. Spatial Distribution of Annual Average (NDVI), (LST), and Rainfall (RF) Value

Based on the MODIS data analysis, the 16 years mean annual estimate of NDVI and LST averaged over the upper Awash Basin is 0.413 and 0.16°C, respectively. A multi-year rainfall data from meteorological stations has a mean annual value of 81.83 mm over the time scale ranging from 2001 to 2015. On the other hand, the western and northwestern part of the sub-basin represents the highest mean value of NDVI and RF, and the lowest mean value of LST. In contrast, the central, eastern and southeastern part of the basin represents the lowest mean NDVI value as a consequence of the relatively low annual mean rainfall and high annual average land surface temperature (Figure 3). Previous study in the same area by [27] supports the results of this study. He reported that areas exhibiting high temperature are characterized by very low vegetation cover and settlement areas. This means, areas that are characterized by low temperature correspond to sparse and densely populated vegetation. There is a spatial variation between NDVI and mean annual rainfall in the Upper Awash Basin, with higher mean annual rainfall corresponding to higher NDVI. In general, lower mean annual LST is coupled with higher NDVI in most parts of the basin.

3.3. Temporal Changes of Kiremit (Main Rainy Season) Mean NDVI, LST, SSTA and RF Value for Upper Awash Basin

Over the study period, the mean value of LST for the kiremit seasons reached highest and lowest values of 27.08°C and 23.37°C in 2009 and 2007, respectively. Whereas, the mean value of the NDVI for the kiremit seasons for the period from 2001 to 2016 has highest and lowest values of 0.67 and 0.59 in 2014 and 2010, respectively. Change curves of kiremit mean NDVI and kiremit mean LST were fluctuating in an opposite direction from 2001 to 2008 and in the same direction from 2008 to 2016 (Figure 4a). On the other hand, the mean values of SST Anomalies (SSTA) for the kiremit season has experienced the highest value of 1.82°C in 2015 and lowest value of -1.19°C in 2010. Also, rainfall during the kiremit season has the highest mean value of 202.33 mm in 2013 and lowest mean value of 145.5 mm in 2002. Change curves of kiremit mean RF and kiremit mean SST Anomalies were fluctuating in an opposite direction in the study period (Figure 4c).

The mean values of SST Anomalies and LST for the kiremit season were declined by 0.02°C and 0.012°C per kiremit season, respectively. On the contrary, the mean values of the NDVI and RF for the same season have increased by 0.001 and 1.007 mm per kiremit season, respectively (Table 2). However, observed trends of mean kiremit NDVI, LST, SSTA and rainfall were not statistically significant (ρ value greater than alpha at 95% confidence interval). This indicates that, Upper Awash Basin is experiencing highly fluctuating climatic variables pattern than its change dimension [54].

3.4. Spatial Distribution of kiremit Average NDVI, LST and RF Value

The sixteen years NDVI values varied from -0.057 to 0.81, LST was deviated from 13.81°C to 30.88°C, and the amount of RF received was between 153.507 mm to 202.565 mm across the basin in kiremit season. Rainfall was highest in northern and western part of the sub-basin and lowest in southern and southeastern part of the region (Figure 5b). The spatial distribution of LST is highest in central, eastern and southeastern part of the region and lowest in northwestern and southwestern part of the region (Figure 5c). An investigation done by [27] has shown that the spatial distribution of LST and NDVI during kiremit season in Upper Awash Basin and he reported that the dark green area represents the dense forest around at the border of Entoto, Chilimo and Menagesh forest, the eastern and southwestern parts of the study area have exhibited high temperature, and the area around the northern parts and some pockets of land in the southern parts exhibit low temperature.

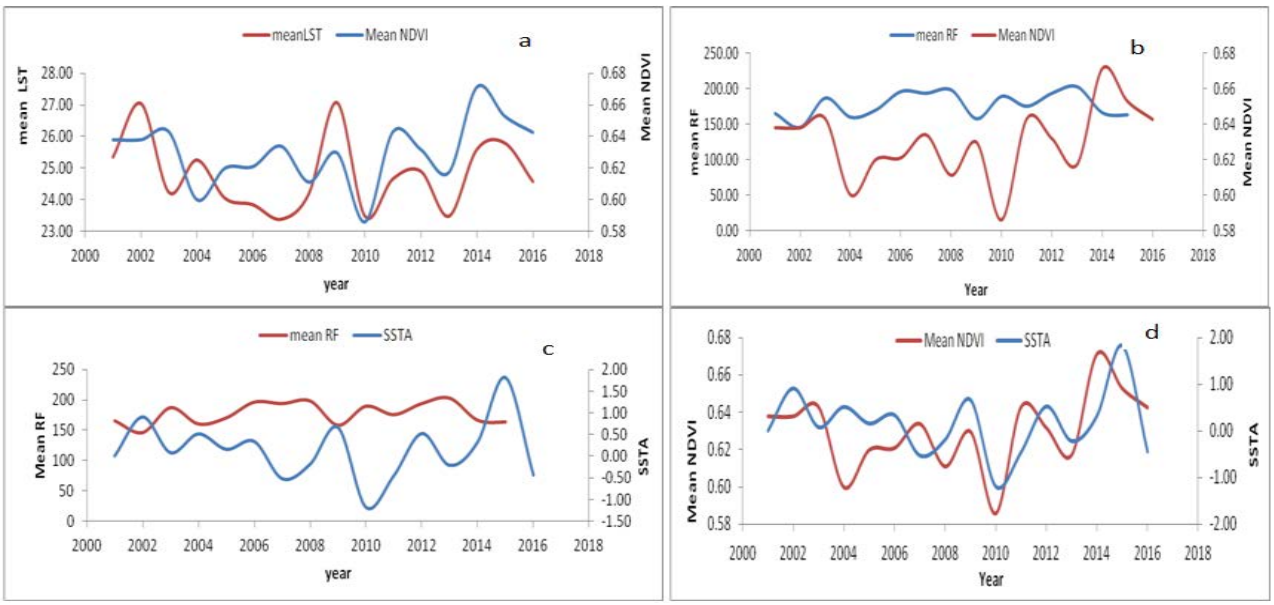

Figure 4. Variation of Kiremt mean LST, NDVI, RF and Mean Kiremt SST Anomalies of the study area from 2000 to 2016

Table 2. Results of the Mann-Kendall trend test for kiremit mean NDVI, LST, SSTA and RF value for Upper Awash Basin

	Kendall's tau	S	*ρ*-value (Two-tailed)	Alpha	Sen's slope
Mean NDVI	0.151	18.000	0.443	0.05	0.001
Mean RF	0.200	21.000	0.328	0.05	1.007
Mean LST	-0.033	-4.000	0.894	0.05	-0.012
SSTA	-0.067	-8.000	0.76	0.05	-0.02

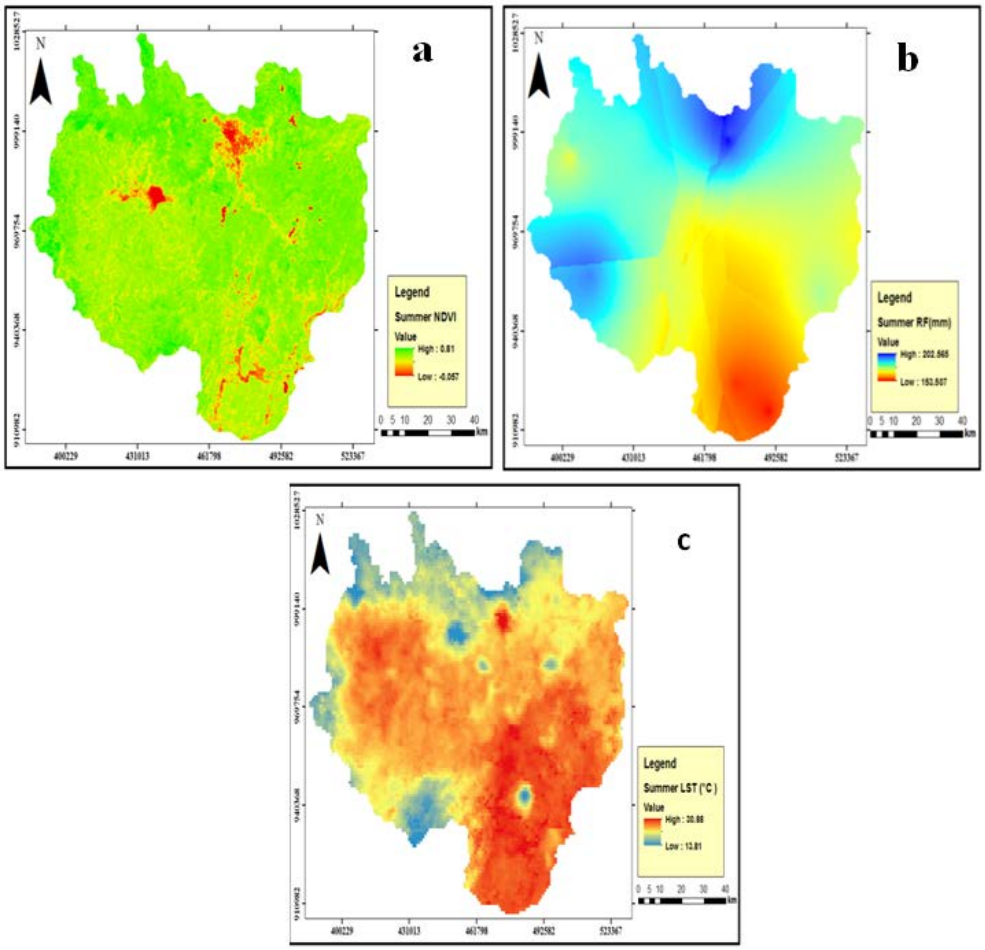

Figure 5. Spatial distribution of the kiremit average NDVI (2001-2016) (a), kiremit average RF (2001-2015) in mm (b) and kiremit average LST (2001-2016) in °C (c) of the Upper Awash Basin

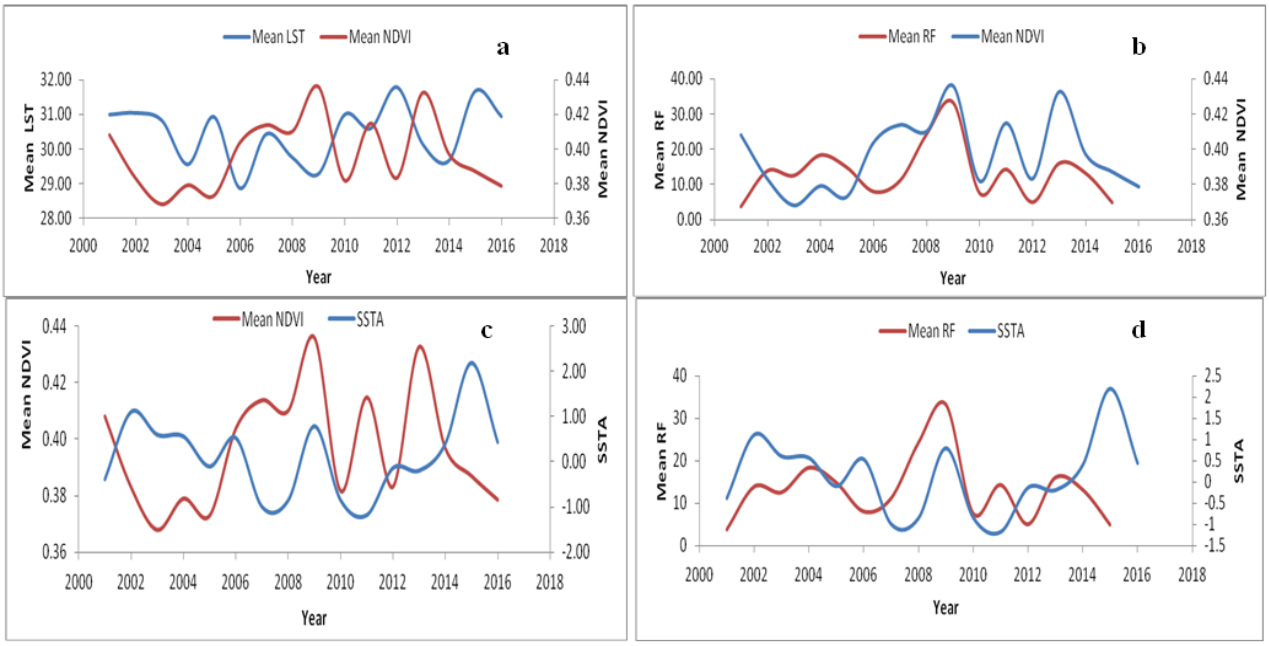

Figure 6. Variation of bega means LST, NDVI, RF and Mean Kiremt SSTA of the study area from 2000 to 2016

Table 3. Results of the Mann-Kendall trend test for bega mean NDVI, LST, SSTA and RF value for Upper Awash Basin

	Kendall's tau	S	ρ-value (Two tailed)	Alpha	Sen's slope
SSTA	-0.050	-6.00	0.82	0.05	-0.01
Mean RF	-0.048	-5.00	0.85	0.05	-0.09
Mean NDVI	0.133	16.0	0.51	0.05	0.00
Mean LST	0.025	3.00	0.93	0.05	0.01

3.5. Temporal Changes of Mean Bega (Dry Season) NDVI, LST, SSTA and RF Value for the Upper Awash Basin

The highest mean bega LST is 31.79°C in 2012 and the lowest mean bega LST is 28.85°C in 2006. The highest mean bega NDVI value is 0.44 in 2009 and the lowest mean bega NDVI value is 0.37 in 2003 (Figure 6a). Over the study period the highest mean bega SSTA is 2.19°C in 2015 and the lowest mean bega SSTA is -1.18°C in 2011. The highest mean bega RF value is 33.28 mm in 2009 and the lowest mean bega RF value is 3.78 mm in 2001 (Figure 6d).

The mean values of SST Anomalies and RF for the bega season showed decrement by 0.01°C and 0.09mm per bega season, respectively. In contrary, the mean values of LST for the bega season have increased by 0.01°C per bega season, but no rate of change for mean values of NDVI were observed during bega season from 2001 to 2016 (Table 3). The Mann-Kendall statistic (S) was -6 for mean bega SSTA and -5 for mean bega RF and it indicates downward trend, while the Mann-Kendall statistic (S) was 16 for mean bega NDVI and 3 for mean bega LST and it indicates upward trend. In addition to this, Table 3 showed that the ρ -values of mean bega NDVI, LST, SST Anomalies and RF is greater than the significance level α (0.05), suggesting that the mean bega rainfall and SST Anomalies decrement and mean bega LST increment was not significant with the confidence level of 95 % over a study period of 2001 to 2016. With regard to the NDVI, no evidence of significant trend was observed, as the computed ρ -values were found to be greater than the critical value at alpha= 0.05.

3.6. Spatial Distribution of Bega Average NDVI, LST and RF Value

The 16 years NDVI value was ranged from -0.1049 to 0.788, LST was distributed from 18.67°C to 36.55°C and RF was distributed from10.91 mm to 17.12 mm across the whole basin in bega season. As shown in Figure 7, the highest NDVI was obtained in western, northwestern and southwestern part of the basin. Highest RF was also recorded in north western part of the basin. The spatial distribution of LST during bega season was highest in eastern and southeastern part of the region and lowest in northern and western part of the basin.

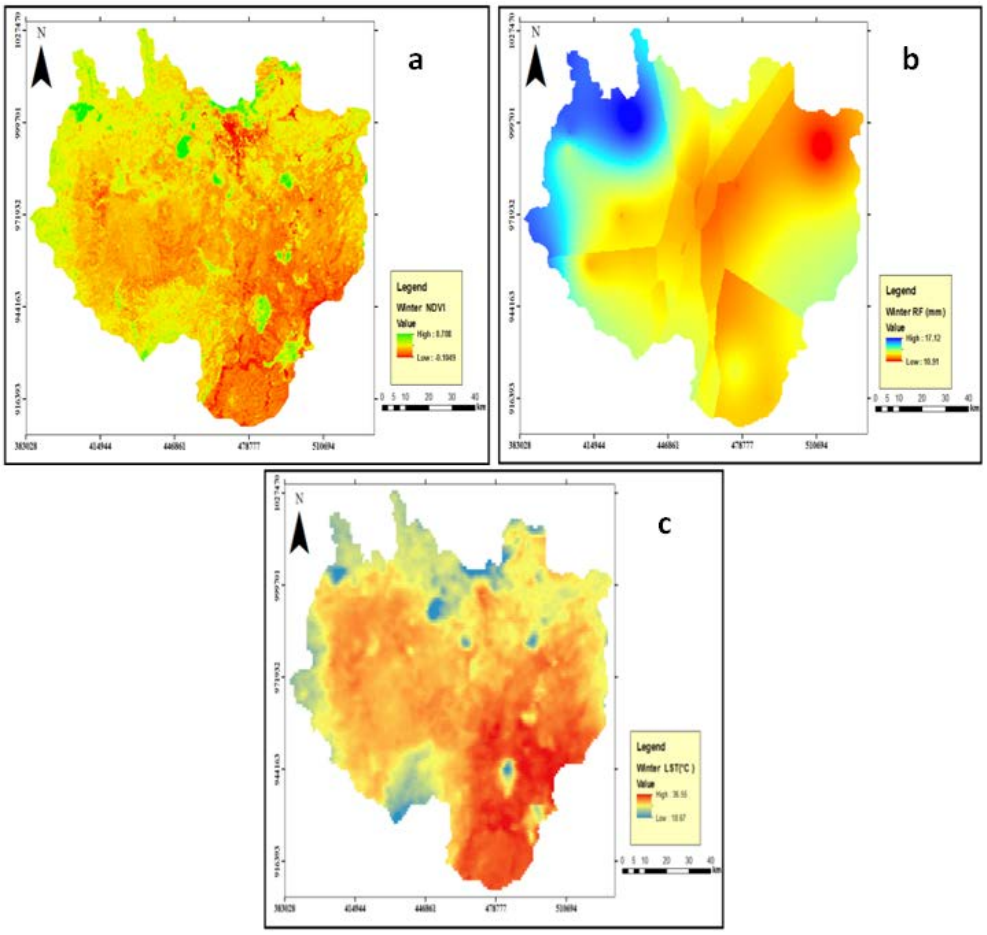

Figure 7. Spatial distribution of bega average NDVI (2001-2016) (a), bega Average RF (2001-2015) in mm (b) and bega Average LST (2001-2016) in °C (c)

3.7. Temporal Changes of belg (short rainy season) Mean NDVI, LST, SSTA and RF Value for the Upper Awash Basin

The results of the temporal analyses revealed that the highest mean belg LST is 37.13°C in 2015 and the lowest mean belg LST is 30.67 °C in 2010. As well, the highest mean belg NDVI value is 0.43 in 2004 and the lowest mean belg NDVI value is 0.26 in 2008 and 2015 (Figure 8a). As indicated in the same figure change curves of belg mean NDVI and belg mean LST were fluctuates almost in opposite direction i.e as the change curve of LST increases, NDVI curve decreases and vice versa. Change curves of belg mean NDVI and belg mean RF were fluctuates almost in the same direction i.e as the change curve of RF increases, NDVI curve also increases (Figure 8b). These changes were not uniform across observation period that there is also minor period where belg NDVI and RF have showed opposite direction of change like from 2004 towards 2007. This opposite direction of change curve of belg NDVI and RF from 2004 to 2007 is an indication of variation in vegetation productivity which is not in connection to variation in precipitation distribution and thus rather linked to other contributing factors that disturbed vegetation growth [57]. The highest mean belg SST Anomalies is 1.37 in 2016 and the lowest mean belg SST Anomalies is -1.17 in 2008 and the highest mean belg RF value is 91.87 mm in 2010 and the lowest mean belg RF value is 27 mm in 2009 (Figure 8c).

As presented in Table 4, the mean values of NDVI and RF for the belg season have decreased by 0.008 and 0.923mm per belg season, respectively. The ρ-value of mean belg NDVI was 0.026. The ρ- values is less than the significance level α (0.05) for mean belg NDVI value, and this suggested that the decrement in the mean value of NDVI was significant with the confidence level of 95 % over a study period of 2001-2016 in belg season. The ρ-value of mean belg RF was 0.559 and it is greater than the significance level α (0.05) suggesting that the belg mean rainfall decrement was not significant with the confidence level of 95 % over a period of 2001-2015. On the contrary, the mean values of LST and SST Anomalies have increased by 0.047°C and 0.029°C per belg season, respectively. The ρ-values of mean values of LST and SSTA are 0.626 and 0.450, respectively for the belg season. Furthermore, ρ - values for LST and SST Anomalies are greater than the significance level α (0.05), suggesting that the increment in LST and SSTA was not significant with the confidence level of 95 % over a study period of 2001-2016.

3.8. Spatial Distribution of belg Average NDVI, LST and RF Value

Results of our analysis showed that the mean values of NDVI (within 16 years period), LST (within 16 years period) and RF (within 15 years period) are 0.33, 34.88°C and 54.63 mm respectively, for the belg season in the Upper Awash Basin. Western and northwestern region of the basin reflects the highest mean NDVI value as a consequence of high belg RF and the low mean LST values. On the other hand The central, eastern and southeastern part of the basin are showing the lowest mean NDVI value as a consequence of the relatively low belg mean rainfall and high belg average land surface temperature.

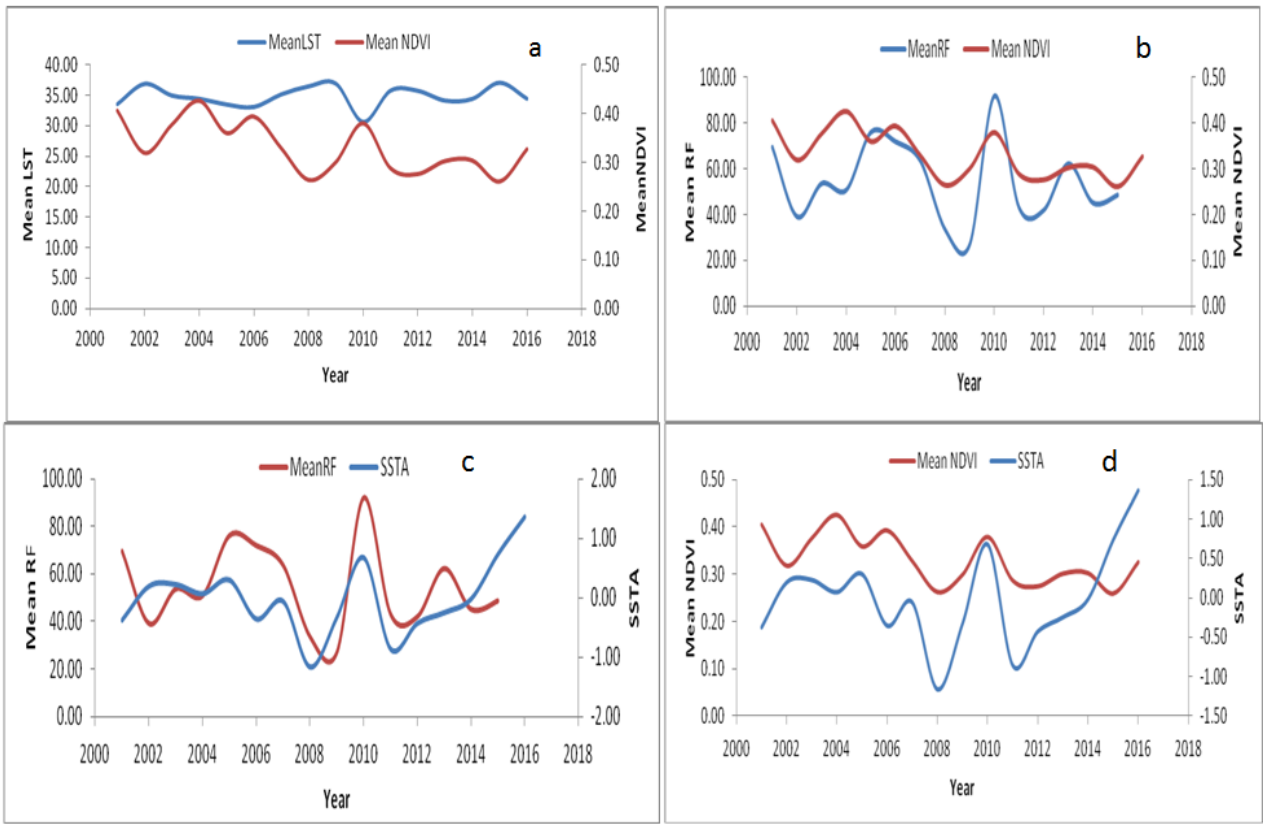

Figure 8. Variation of belg means LST, NDVI, RF and SST Anomalies of the Upper Awash Basin from 2001 to 2016

Table 4. Results of the Mann-Kendall trend test for belg mean NDVI, LST, SSTA and RF value for Upper Awash Basin

	Kendall's tau	S	*p*-value(Two-tailed)	Alpha(α)	Sen's slope
Mean NDVI	-0.417	-50.0	0.026	0.05	-0.008
Mean LST	0.100	12.0	0.626	0.05	0.047
SSTA	0.150	18.0	0.450	0.05	0.029
Mean RF	-0.124	-13.0	0.559	0.05	-0.923

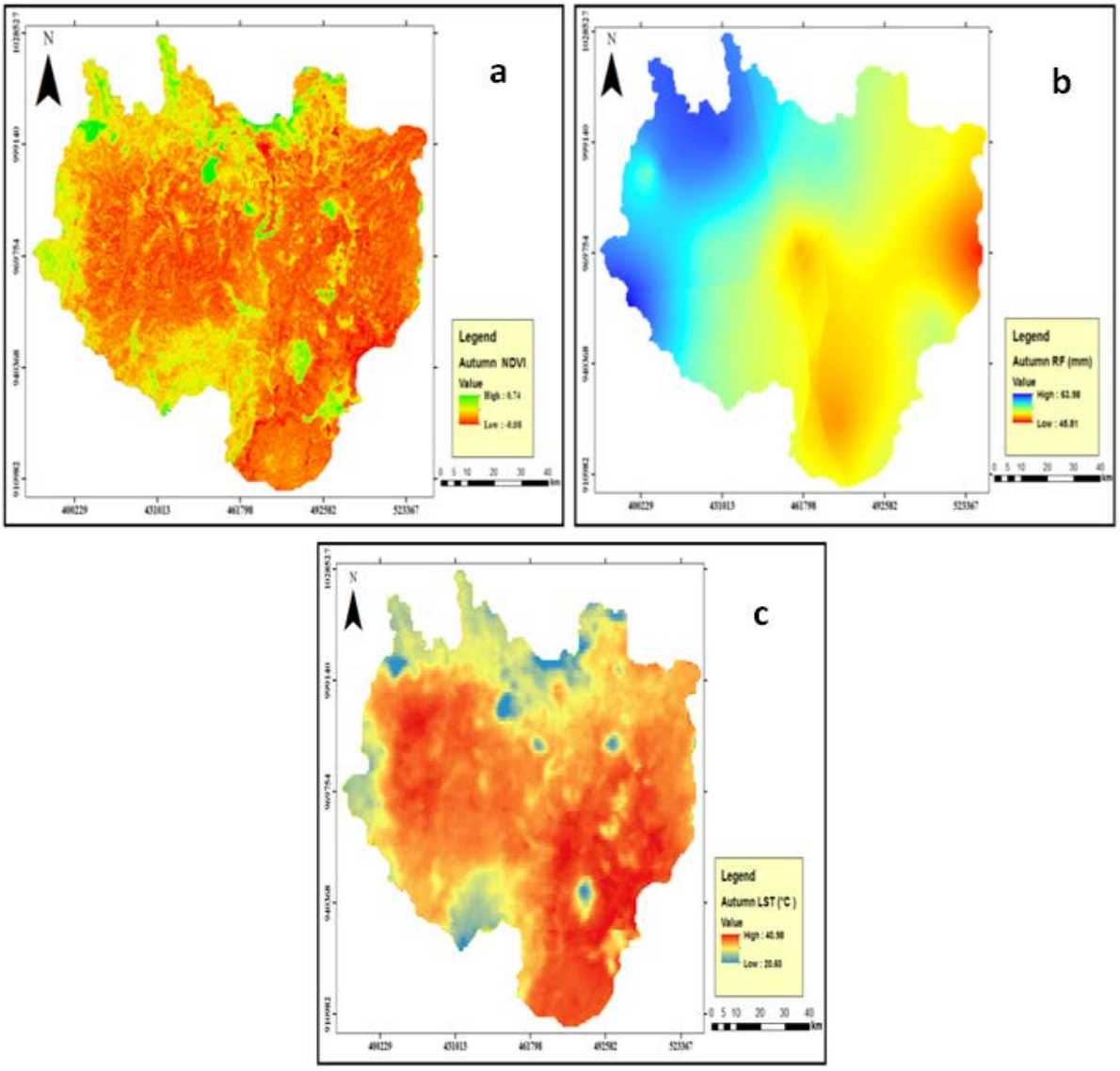

Figure 9. Spatial distribution of the belg average NDVI (2001-2016) (a), belg average RF (2001-2015) in mm (b) and belg average LST (2001-2016) in °C (c)

3.9. Association between NDVI and Climatic Elements

Evaluating the associated climatic elements with NDVI is of prime importance to understand how these determinant factors affect the vegetation biomass. For instance, the availability and distribution of rainfall is among the determinant factors for plant productivity in semi-arid regions [58]. Additionally, other factors like temperature, evapotranspiration and soil properties can affect the growth of dry land vegetation [59]. Precipitation and temperature directly influence water balance, causing changes in soil moisture regime which in turn, influences plant growth [18].

3.9.1. Association between Annual NDVI and Annual Climatic Elements

Strong positive association between NDVI and rainfall over different regions has been reported from earlier studies [17,18,60,61,62]. Similarly, this study show that the correlation between annual average NDVI and annual mean rainfall in the Upper Awash basin was positive (r=0.51) with a significance level alpha 0.05. [63] and [64] also reported the existence of positive correlation between annual NDVI and annual rainfall. They reported that rainfall enhanced the vegetation growth. Similar to finding of this research [65] have also claimed the positive correlations between NDVI and RF in Northeastern Brazil and showed the enhancement of vegetation growth by rainfall.

Table 5. Correlation coefficients between NDVI and climatic elements and, between SST Anomalies and RF in Upper Awash Basin

	NDVI vs RF		NDVI vs LST		NDVI vs SSTA		RF vs SSTA		LST vs SSTA	
	r	ρ	r	ρ	r	ρ	R	ρ	r	ρ
Annual	0.51	0.05	-0.58	0.02	-0.41	0.12	-0.56	0.03	0.57	0.02
Kiremit	-0.33	0.22	0.41	0.11	0.42	0.11	-0.56	0.03	0.69	0.00
Bega	0.45	0.09	-0.50	0.05	-0.29	0.27	-0.02	0.95	0.07	0.80
Belg	0.62	0.01	-0.67	0.00	0.22	0.42	0.46	0.09	-0.27	0.31

The correlation between mean annual values of NDVI and LST is negative (r= -0.58) with a significance level alpha 0.05. Similar to the finding of this study, [61] have claimed the negative correlation between NDVI and temperature over Tibetan Plateau from 1980 to 2002. This implies that, higher temperature causes an increased evaporation, and consequently, a lower plant production. In general, many studies have reported the negative correlation between temperature and vegetation growth. The higher LST increases plant respiration and reduce net photosynthesis that ultimately results in reduced crop yield. USWCL [66] showed that the temperature of the canopy is related to plant water stress magnitude. This relation is based on the mechanism, by which plants transpire water in order to cool their leaves. When there is no enough water, transpiration is reduced and leaf temperature is increased. Hence moderate negative correlation between mean annual NDVI and annual average LST indicated that the degree of relation between NDVI and LST is an inverse one. The study has also indicated that LST constrains vegetation growth.

The association between annual values of NDVI and SST Anomalies across the Upper Awash Basin is low negative (r = -0.41) with a significant value of alpha 0.05. Similar magnitude of negative correlation was also reported by [67] between NDVI and Niño 3 SST Anomalies over east and southern Africa. These results show the negative impact of ENSO on vegetation growth. During La Niña years, the amount of mean annual NDVI was higher than El Niño years. That is, the mean annual value of NDVI during La Niña (0.41 in 2008 and 0.41 in 2011) is higher than its mean annual value (0.40 in 2002 and 0.39 in 2015) during El Niño years.

3.9.2. Association between Seasonal NDVI and Seasonal Climatic Elements

The strong positive correlations between NDVI and rainfall (r=0.62) in belg season indicates that the availability of rainfall is one of the major factors that determine the density of vegetation (Table 5). However, low positive correlation (r=0.45) was obtained for bega season. Low negative correlation (r = -0.33) was also attained in kiremit season. The negative correlation between rainfall and NDVI in kiremit season could be due to signal saturation above certain biomass values, to a deficit of solar radiation used for the photosynthesis because of cloud [68,69]. Some scholars have shown that the large amount of rainfall increases the amount of clouds, which reduces the solar radiation and decreases the temperature [70,71]. Additionally, due to heavy rains that manifest the higher rates of run-off, particularly when soil is moist [64]. Thus, in the Upper Awash basin, increased precipitation during kiremit season can lead to increase cloud cover, which inhibits vegetation growth to some extent. The correlation between NDVI and RF in belg season is higher than kiremit and bega season. This indicated that the contribution of RF in vegetation coverage increment is higher in belg season than kiremit and bega seasons.

The correlation between NDVI and LST was positive (r=0.414) in kiremit, and negative in bega and belg corresponding to (r = -0.50) and (r= -0.67), respectively in the Upper Awash Basin. However, climate-vegetation relationship is complex with nonlinear characteristics. Specifically, before the optimum temperature for photosynthesis, a temperature rise will enhance vegetation growth by an accelerated release of nutrients and improved availability from the soil [72]. Similar results were observed, in the Upper Awash Basin during kiremit season. When temperature significantly increases, however, the respiration will be increased and accelerated the nutrients consumption, especially in the effect regions of negative temperature-vegetation relationship [72] and this observed in the bega and belg season for the case of Upper Awash Basin. The correlation between NDVI and LST in belg season is higher than kiremit and bega season. This indicates that the influence of LST on vegetation coverage is higher in belg season than kiremit and bega season.

The correlation between seasonal NDVI and Niño 3.4 SST Anomalies was negative in bega (r = - 0.29) and positive in kiremit and belg accounting for (r = 0.42) and (r=0.22) correlation coefficients, respectively (Table 5). In belg (short rainy season and kiremit (main rainy season) SST Anomalies have positive correlation with NDVI, but the contribution of SST Anomalies on NDVI was higher in the main rainy season than the short rainy season in Upper Awash Basin. On the contrary, in dry season (bega) Niño 3.4 SSTA and NDVI has negative correlation, but the contribution is not substantial. Similar to the findings of this study, [73] have claimed positive correlation between ENSO (Niño 3.4 SSTA) and NDVI in belg season over northwestern Africa.

The amount of mean belg NDVI was higher during El Niño than La Niña. The mean belg NDVI (0.26 in 2008 and 0.29 in 2011) during La Niña was less than mean belg NDVI (0.32 in 2002 and 37.13 in 2015) corresponding to El Niño years. Similarly, the amount of mean kiremit NDVI was almost higher during El Niño than La Niña. The mean kiremit NDVI (0.61 in 2008 and 0.63.99 in 2011) during La Niña was less than mean kiremit NDVI (0.64 in 2002 and 0.65 in 2015) of El Niño years. In contrast, during La Niña years the amount of mean bega NDVI was higher than El Niño years. The mean bega NDVI (0.41 in 2008 and 0.41 in 2011) determined during the La Niña was higher than the corresponding values of mean bega NDVI (0.38 in 2002 and 0.39 in 2015) obtained for the El Niño period.

On the other hand, the correlation between mean annual values of rainfall and SST Anomalies was generally negative (r = -0.56). Similarly, the correlation between mean values of rainfall and SST Anomalies was generally negative in kiremit (r = -0.56) and bega (r= -0.02) and positive in belg(r=0.46) (Table 5). Similar to the findings of current study, an empirical study undertaken by [17] reported that SST Anomalies increases the amount of rainfall in belg season. Other similar study made by [54] showed that the correlation between SST Anomalies and RF was negative and positive in kiremit and belg seasons, respectively in Upper Awash Basin. This study shows positive contribution of SST Anomalies in belg season is higher than kiremit and bega seasons. Whereas, SST Anomalies and rainfall has moderate negative correlation in kiremit season. The results of this study indicate that SST Anomalies adversely affects rainfall distribution in kiremit season than bega and belg seasons. As described by [74] the amount of rainfall in La Niña years was higher than El Niño years. Similar result was obtained in this study, and the amount of mean annual rainfall was higher in La Niña years (85.28mm in 2008 and 77.56mm in 2011) than El Niño years (66.24mm in 2002 and 72.21mm in 2015). During La Niña years, the amount of mean rainfall in kiremit season was also higher than El Niño years. Mean kiremit rainfall (197.84mm in 2008 and 175.09mm in 2011) during La Niña was higher than mean kiremit rainfall (145.50mm in 2002 and 162.99mm in 2015) in El Niño years. On the contrary, the amount of mean belg rainfall was higher in El Niño than La Niña years. Mean belg rainfall (33.69mm in 2008 and 43.18mm in 2011) in La Niña years was less than mean belg rainfall (39.23mm in 2002 and 48.67mm in 2015) during El Niño years. Similar, finding was reported by [17] in Gojjam, Ethiopia.

4. Conclusion

Quantifying the spatio-temporal pattern of vegetation dynamics and climatic variables at the regional scale is critical to provide a theoretical basis for evaluating the interaction between climate variability and vegetation dynamics. There is spatio-temporal variation of vegetation cover as a consequence of main climatic elements variability (RF and LST) and SST Anomalies in the study area. The Mann-Kendall trend test shows that there is no significant trend in the annual and seasonal NDVI, LST, SST Anomalies and rainfall variability over the basin during the period 2001 to 2016, except NDVI values in belg season. The contribution of RF in vegetation coverage enhancement is higher in belg season than kiremit and bega seasons. The negative impact of LST on vegetation coverage is also higher in belg season than kiremit and bega season. The amount of vegetation coverage and rainfall were higher during El Niño episode than La Niña episode in belg season. Similarly the amount of vegetation coverage in kiremit season was almost higher during El Niño years than La Niña years. On the other hand during La Niña years, the amount of rainfall in kiremit season was higher than El Niño years in the study area. As a concluding remark two issues has been recommended. El Nino episode increases the amount of rainfall in belg season. It is advisable for farmers to sow belg crops during El Nino episode. It will be good to integrate population dataset for in depth analysis of the role of population dynamics and pressure as drivers of vegetation changes indicated by the NDVI.

Acknowledgments

The success of this research would not have been possible without the financial support from Haramaya University, which is gratefully acknowledged. Moreover I would like to extend my gratitude to the Entoto Observatory and Research Center (EORC) and Oda Bultum University for providing additional funds for the field research and publication.

References

[1] Rechid, D, (2008). On biogeophysical interactions between vegetation phenology and climate simulated over Europe, Max Planck Institute for Meteorology.

[2] Cao, M., and Woodward. F.I. (1998). "Dynamic Responses of Terrestrial Ecosystem Carbon Cycling to Global Climate Change." Nature 393: 249-252.

[3] Pielke, R. A., R. Avissar, M. Raupach, A. J. Dolman, X. Zeng, and A.S. Denning. (1998). "Interactions between the Atmosphere and Terrestrial Ecosystems: Influence on Weather and Climate." Global Change Biology 4:461 475.

[4] Suzanvander K.S, (2009). Quantifying vegetation cover changes from NDVI time series and determination of main causes for the Nile Basin, Master thesis, Delft University of Technology.

[5] Wang, G.X.; Bai, W.; Li, N.; Hu, H.C (2011**)**. Climate changes and its impact on tundra ecosystem in Qinghai-Tibet Plateau, China. *Clim. Change* 2011, *106*, 463-482.

[6] Zavaleta, E. S., M. R. Shaw, N. R. Chiariello, H. A. Mooney, and C. B. Field. (2003). "Additive Effects of Simulated Climate Changes, Elevated CO2, and Nitrogen Deposition on Grassland Diversity." Proceedings of the National Academy of Sciences of the United State of America.

[7] Rees, M., R. Condit, M. Crawley, S. Pacala, and D. Tilman. (2001). "Long-Term Studies of Vegetation Dynamics."Science 293: 650-655.

[8] Ogunbadewa, E. (2013). Climatic Variability Prediction with Satellite Remote Sensing and Meteorological Data in the South Western Nigeria. Geodesy and Cartography, Volume 39(2): 59-63.

[9] Zhong L., Yaoming Ma, Mhd. Suhyb Salama and Zhongbo Su (2010). Assessment of vegetation dynamics and their response to variations in precipitation and temperature in the Tibetan Plateau. Climatic Change, 103: 519-535.

[10] Ahl, D., Gower, S., Burrows, S., Shabanov, N., Myneni, R., Knyazikhin, Y. (2006). Monitoring spring canopy phenology of a deciduous broad leaf forest using MODIS. *Remote Sensing of Environment* 104(1), 88-95.

[11] Kulawardhana, R.W.(2008). Determination of spatio-temporal variations of vegetation cover, land surface temperature and rainfall and their relationships over Sri 59 Lanka using NOAA AVHRR data. Master's Thesis, University of Peradeniya, Department of Agricultural Engineering, Sri Lanka.

[12] Roerink, G.J., Menenti, M., Soepboer, W. & Su, Z. (2003). Assessment of climate impact on vegetation dynamics by using remote sensing. Phys. Chem. Earth 28, 103-109.

[13] Zhang, G.; Zhang, Y.; Dong, J.; Xiao, X. (2013). Green-up dates in the Tibetan plateau have continuously advanced from 1982 to 2011. *Proc. Natl. Acad. Sci.* 2013, *110*, 4309-4314.

[14] Kandji ST, Verchot L, Mackensen J (2006). Climate Change, Climate and Variability in Southern Africa: Impacts and Adaptation in the Agricultural Sector. Word Agro forestry Centre (ICRAF), United Nations Environment Programme (UNEP), Nairobi, Kenya, pp. 42.

[15] Mikias Biazen, (2014). The Effect of Climate Change and Variability on the Livelihoods of Local Communities: In the Case of Central Rift Valley Region of Ethiopia.

[16] Korech D; Barnston A (2007). Predictability of June- September Rainfall in Ethiopia, Am Meteorol Soc 135:628-650.

[17] Getahun YS and Shefne BG (2015). Analysis of Climate Variability (ENSO) and Vegetation Dynamics in Gojjam, Ethiopia. J Earth Sci Clim Change. 6: 320.

[18] Souleymane S. (2015). Long -Term Vegetation Dynamics over the Bani River Basin as Impacted by Climate Change and Land Use, PhD thesis, Kwame Nkrumah University of science and Technology, Kumasi

[19] Hengl, T. (2009). A Practical Guide to Geostatistical Mapping. Luxembourg: Office for Official Publications of the European Communities.

[20] Jantakat, Y., and Ongsomwang, S., (2011). Assessing the effect of incorporating topographical data with geostatistical interpolation for monthly rainfall and temperature in Ping Basin, Thailand. *Suranaree Journal of Science and Technology* 18(2), 123-139.

[21] Ly, S., Charles, C. and Degr, A. (2011). Geostatistical Interpolation of Daily Rainfall at Catchment Scale; The Use Of Several Variogram Models in the Ourthe and Ambleve Catchments, Belgium. *Hydrology and Earth System Science, 15*, 2259-2274.

[22] Mair, A. and Fares, A. (2011). Comparison of Rainfall Interpolation Methods in a Mountainous Region of aTropical Island. *Journal of Hydrologic Engineering*, 371- 383.

[23] ITC-ILWIS (2001). Geostatstics in ILWIS 3.0 Academic User's Guide. International Institute for Aerospace Survey and Earth Sciences (ITC) Enschede, the Netherlands.

[24] Babu., A. (2009). "The impact of Pacific sea surface temperature on the Ethiopian rainfall". Workshop on High Impact Weather Predictability Information Systemfor Africa and AMMA THORPEX Forecasters. Trieste, Italy: National Meteorological Agency.

[25] Zaroug, M. (2010), "The connections of Pacific SST and drought over East Africa". *DEWFORA meeting at ECMWF*, Improved Drought Early Warning and FORecasting to strengthen preparedness and adaptation to droughts in Africa (DEWFORA), United Kingdom, 4-5 October

[26] Justice, C., and Townshend, J. (2002). Special issue on the moderate resolution imaging Spectro -radiometer (MODIS): A new generation of land surface monitoring, Remote Sensing of Environment 83.

[27] Tesfamariam .E, (2016). Characterizing the Hydro-climatic Deficient Moisture to Monitor Agricultural Drought by Using Remote Sensing:The Case of Upper Awash Basin, Ethiopia, Entoto Observatory and Research Center, Master thesis, Addis Ababa University.

[28] CHEN Yun-Hao, LI Xiao-Bing, SHI Pei-Jun.(2003). Intra- annual Vegetation Change Characteristics in the NDVI- Ts Space: Application to Farming-Pastoral Zone in North China, Acta Botanica Sinica, 2003, 45 (10): 1139-1145.

[29] Huete, A.R., and Liu, H.Q., (1994). An error and sensitivity analysis of the atmospheric- and soil correcting variants of the NDVI for the MODIS-EOS, *IEEE Transactions on Geoscience and Remote Sensing*, 32, pp. 897-905.

[30] Xiao, X.M., Braswell, B., Zhang, Q.Y., Boles, S., and Frolking, S. (2003). Sensitivity of vegetation indices to atmospheric aerosols: continental-scale observations in northern Asia. *Remote Sensing of Environment*, 84, pp. 385-392.

[31] Lu, X., Liu, R., and Liang, S. (2007). Removal of noise by wavelet method to generate high quality temporal data of terrestrial MODIS products. *Photogrammetric Engineering and Remote Sensing*, 73, pp. 1129-1139.

[32] Jonsson, P and Eklundh, L. (2002). Seasonality extraction by function fitting to time-series of satellite sensor data. *IEEE Trans Geosci Remote Sens.* 2002, *40*, 1824-1832.

[33] Beck, P. S. A., Atzberger, C., and Hogda, K. A.(2006). Improved monitoring of vegetation dynamics at very high latitudes, a new method using MODIS NDVI. Remote Sensing of Environment, vol. 100, pp. 321-336.

[34] Ren, J., Chen, Z., Zhou, Q., and Tang, H.(2008). Regional yield estimation for winter wheat with MODIS-NDVI data in Shandong, China.International Journal of Applied Earth Observation and Geoinformation, vol.10(2008), pp.403-413.

[35] Brooks, E.B., Thomas, V.A., Wynne, R.H., Coulston, J.W. (2012). Fitting the multitemporal curve: A Fourier series approach to the missing data problem in remote sensing analysis. *IEEE Trans. Geosci. Remote Sens*. 2012, *50*, 3340-3353.

[36] Ephraim. R.L. (2015). Time Series Analysis of MODIS NDVI data with Cloudy Pixels: Frequency-domain analyses of vegetation change in Western Rwanda, Master thesis, *University of Tennessee.*

[37] Ermias T.D. (2015). Soil hydrological impacts and climatic controls of land use and land cover changes in the Upper Blue Nile (Abay) basin. PhD Thesis, Delft University of Technology.

[38] Zhou, J.; Li, J; Menenti, M. (2015). Reconstruction of global MODIS NDVI time series: Performance of Harmonic Analysis of Time Series (HANTS). *Remote Sens. Environ.* 2015, *163*, 217-228.

[39] Souleymane S.T, Tobias L, Eric K. F and Pierre C.S. T (2014). Assessing Long-Term Trends in Vegetation Productivity Change over the Bani River Basin in Mali (West Africa), Journal of Geography and Earth Sciences December 2014, Vol. 2, No. 2, pp. 21-3.

[40] Ndiritu, J. G., (2005). Long-term trends of heavy rainfall in South Africa. Regional hydrological Impacts of Climate Change-Hydroclimativ Variability. In: Proceedings of symposium S6 held during seventh IAHS Scientific Assembly at Foz do Iguacu, Brazil, April 2005. IAHS Publ. 296, pp. 178-183.

[41] Burns, D. A., Klaus, J., and McHale, M. R.(2007). Recent climate trends and implications for water resources in the Catskill Mountain region, New York, USA. Journal of Hydrology, vol. 336(1-2), pp. 155-170.

[42] He Y, Thomas U, Rasmus F, Dirk P and Patrick H (2012). How Normalized Difference Vegetation Index (NDVI) Trends from Advanced Very High Resolution (AVHRR) and Système Probatoired'Observation de la Terre VEGETATION (SPOT VGT) Time Series Differ in Agricultural Areas: An Inner Mongolian Case Study. *Remote Sens.* 2012, *4*, 3364-3389.

[43] Changbin L.; Jiaguo Q.;, Linshan Y.; Shuaibing W; Wenjin Y;, Gaofeng Z; Songbing Z;and Feng Z.(2014). Regional vegetation dynamics and its response to climate change,a case study in the Tao River Basin in Northwestern China, Environmental Research Letters, vol. 300, pp.1560-1563.

[44] Udelhoven, T. (2011**)**. Time Stats: A software tool for the retrieval of temporal patterns from global satellite archives. *IEEE J. Sel. Top. Appl. Earth Obs. Remote Sens.* 2011, *4*, 310-317.

[45] Nayak A, Marks D, Chandler D G and Seyfried M (2010). Long-term snow, climate, and stream flow trends at the reynolds creek experimental watershed, Owyhee Mountains, Idaho, United States Water Resour. Res. 46 W06519.

[46] Yin H; Li Z G; Wang Y L and Cai F. (2011). Assessment of desertification using time series analysis of hyper- temporal vegetation indicator in Inner Mongolia Acta Geographica Sin. 66 653-61 (in Chinese).

[47] Bouza-Deano, R., Ternero-Rodriguez, M., Fernandez- Espinosa, A.J.(2008). Trend study and assessment of surface water quality in the Ebro River (Spain). *J. Hydrol.* 2008, *361*, 227-239.

[48] Donald W. Meals, Jean Spooner, Steven A. Dressing, and Jon B. Harcum. (2011). Statistical analysis for monotonic trends, Tech Notes 6, November 2011. Developed for U.S.Environmental Protection Agency by Tetra Tech, Inc., Fairfax, VA, 23 p.

[49] GUO W, NI X, JING D, Shuheng L,(2014). Spatial-temporal patterns of vegetation dynamics and their relationships to climate variations in Qinghai Lake Basin using MODIS time series data, Journal of Geographical Sciences J. Geogr. Sci. 2014, 24(6): 1009-1021.

[50] Xu Jianhua. (2002). Mathematical Methods in Contemporary Geography. Beijing: High Education Press. (In Chinese).

[51] Mu Shaojie, Yang Hongfei, Li Jianlong *(*2013). Spatio- temporal dynamics of vegetation coverage and its relationship with climate factors in Inner Mongolia, China. *Journal of Geographical Science*, 23 (2): 231-246.

[52] Yohanis T. (2012). Evapotranspiration using geontcast in-situ data streams for drought monitoring and early warning. M.sc thesis, ITC, netherlands.

[53] Mirko G, Brigitta S, Gerd F (2010) Spatiotemporal Variability of Land Use and Land Cover in the Abaya - Chamo-Basin, Southern Ethiopia since 1981

[54] Abdisa, A. (2015). Seasonal climate prediction for rain-fed crop production planning in the Upper Awash Basin , central high land of Ethiopia, Master thesis , Haramaya University.

[55] Gezahagn N. S.(2016). Spatial Assessment of NDVI as an Indicator of Desertification in Ethiopia using Remote Sensing and GIS, Master Thesis, Lund University,

[56] Seleshi,Y.and Zanke,U. (2004). Recent changes in rainfall and rainy days in Ethiopia. *International Journal of Climatology*, *24*(8), 973-983.

[57] Worku Z. G. (2016). Climate, land use and vegetation trends: implication of land use change and climate change on Northwestern dry land of Ethiopia, PhD thesis Dresden University, Dresden.

[58] Wang, J., Price, K. P.,and Rich, P. M. (2001). Spatial patterns of NDVI in response to precipitation and temperature in the central Great Plains. *International Journal of Remote Sensing*, *22*, 3827-3844.

[59] Ji, L., and Peters, A. J., (2004). A spatial regression procedure for evaluating the relationship between AVHRR- NDVI and climate in the northern Great Plains. *International Journal of Remote Sensing*, *25*, 297-311.

[60] Wang, J., Price, K. P.and Rich, P. M., (2003). Temporal responses of NDVI to precipitation and temperature in the central Great Plains, USA. Int. J. Remote Sensing, 24 (11): 2345-2364.

[61] Jian S, Genwei C, Weipeng L, Yukun S and Yunchuan Y. (2013). On the Variation of NDVI with the Principal Climatic Elements in the Tibetan Plateau *Remote Sens.* 2013, *5*, 1894-1911.

[62] Jiangbo G, Kewei J, Shaohong W, Danyang M, Dongsheng Z, Yunhe Y, and Erfu D. (2017). Past and future influence of climate change on spatially heterogeneous vegetation activity in China Earth Syst. Dynam. Discuss. 2017.

[63] Esubalew. N.B. (2014). GIS and Remote Sensing techniques application to the spatio-temporal climatic variability analysis the case of Ziway Dugda and Dodota Woreda, Arsi Zone, Oromia Region, Ethiopia, Master thesis , Addis Ababa University.

[64] Humberto A. Barbosa and T. V. Lakshmi Kumar (2012). Strengthening Regional Capacities for Providing Remote Sensing Decision Support in Drylands in the Context of Climate Variability and Change, International Perspectives on Global Environmental Change, Dr. Stephen Young (Ed.), InTech,

[65] Stefan E., Anne S., Marx P. B. and Joerg M. (2014). Vegetation Greenness in Northeastern Brazil and Its Relation to ENSO Warm Events, *Remote Sens.* 2014, *6*, 3041-3058.

[66] USWCL, (2001). Thermal crop water stress index. U.S. water conservation laboratory, phoenix, Arizona, from http://www.plant stress.com/article/drought.

[67] Anyamba, A., Tucker, C. J. and Mahoney, R. (2002). From El Niño and La Nina: Vegetation response patterns over East and Southern Africa during 1997-2000 period, *J. Climate*, 15, 3096-3103.

[68] Camberlin, P., Martiny, N., Philippon, N., Richard, Y. (2007). Determinants of the inter annual relationships between remote sensed photosynthetic activity and rainfall in tropical Africa, Remote Sensing of Environment, 106, 199-216.

[69] Song, Y., and Ma, M. G., 2008. Variation of AVHRR NDVI and its relationship with climate in Chinese arid and cold regions. Journal of Remote Sensing, vol. 12(3), pp. 499-505.

[70] Zhang, Y. H., Fan, G. Z., Li, L. P., Zhou, D. W., Wang, Y. L., and Huang, X. L. (2009). Preliminary analysis on the relationships betwee NDVI change and its temperature and precipitation in southwest China. *Plateau and Mountain Meteorology Research*, 29(1), 6-13. (in Chinese)

[71] Jun DU, Chang-xing S, Chen-di Z. (2013). Modeling and analysis of effects of precipitation and vegetation coverage on runoff and sediment yield in Jinsha River Basin. *Water Scienc and Engineering*, 2013, 6(1): 44-58.

[72] Michaletz, S. T., Cheng, D., Kerkhoff, A. J., and Enquist, B. J. (2014). Convergence of terrestrial plant production across global climate gradients, Nature, 512, 39-43.

[73] Nathalie P., Aur´elie B., Nad`ege M., Pierre C., Timm H., (2012). Timing and patterns of ENSO impacts in Africa over the last 30 years insights from Normalized Difference Vegetation Index data. 2012.

[74] Rajashree, V. and Yashwant B., l. (2014). Response of Rainfall and Vegetation to ENSO Events during 2001-2011 in Upper Wardha Watershed, Maharashtra, India, J. Hydrol. Eng., 2014, 19(3): 583-592.